A Photoelectrochemical Device with a Nanostructured SnO_2 Electrode Modified with Composite Clusters of Porphyrin-Modified Silica Nanoparticle and Fullerene

Hiroshi Imahori,*,†,# Keigo Mitamura,† Yuki Shibano,† Tomokazu Umeyama,† Yoshihiro Matano,† Kaname Yoshida,‡ Seiji Isoda,‡ Yasuyuki Araki,¶ and Osamu Ito¶

Department of Molecular Engineering, Graduate School of Engineering, Kyoto University, Nishikyo-ku, Kyoto 615-8510, Japan, Fukui Institute for Fundamental Chemistry, Kyoto University, 34-4, Takano-Nishihiraki-cho, Sakyo-ku, Kyoto 606-8103, Japan, Institute for Chemical Research, Kyoto University, Uji, Kyoto 611-0011, Japan, and Institute of Multidisciplinary Research for Advanced Materials, Tohoku, Katahira, Aoba-ku, Sendai 980-8577, Japan

Received: March 13, 2006; In Final Form: April 15, 2006

A silica nanoparticle has been successfully employed as a nanoscaffold to self-organize porphyrin and C_{60} molecules on a nanostructured SnO_2 electrode. The quenching of the porphyrin excited singlet state on the silica nanoparticle is suppressed significantly, showing that silica nanoparticles are promising scaffolds for organizing photoactive molecules three-dimensionally in nanometer scale. Marked enhancement of the photocurrent generation was achieved in the present system compared with the reference system, where a gold core was employed as a scaffold of porphyrins instead of a silica nanoparticle. The rather small incident photon-to-current efficiency relative to a similar photoelectrochemical device using a silica microparticle may result from poor electron and hole mobility in the composite film due to poor connection between the composite clusters of a porphyrin-modified silica nanoparticle and C_{60} in micrometer scale.

Introduction

Organic-based photovoltaic devices, including dye-sensitized and bulk heterojunction solar cells, have attracted considerable attention due to their potential for low cost, environment-friendly solar energy conversion.[1−8] Supramolecular self-organization of donor (D) and acceptor (A) molecules on electrodes is a promising methodology for attaining both efficient charge separation and subsequent electron and hole transportation in the films on the electrodes. Recently, Fukuzumi et al. and we have successfully constructed a novel type of supramolecular organic solar cells (dye-sensitized bulk heterojunction type),[9] which possesses both characteristics of the organic solar cells. Namely, porphyrins are three-dimensionally organized using scaffolds of dendrimers,[10] oligomers,[11] and nanoparticles[12,13] (1st step). These porphyrin molecular assemblies form supramolecular complexes with C_{60} molecules in toluene due to the $\pi-\pi$ interaction (2nd step),[14] and they are associated with growing larger composite clusters in acetonitrile/toluene mixed solvent due to the lyophobic interaction (3rd step). Then, the large composite clusters can be assembled as three-dimensional D−A interpenetrating arrays onto nanostructured SnO_2 electrodes to afford the SnO_2 electrodes modified with the composite clusters of the porphyrin and C_{60} molecules using an electrophoretic deposition method (4th step).[15] Specifically, the bottom-up self-assembled film of the composite clusters using gold nanoparticles exhibited efficient photocurrent generation relative to the related systems.[16] However, drawbacks of utilizing gold nanoparticles as nanoscaffolds are expensive cost and strong energy transfer (EN) quenching of the porphyrin excited singlet state by the gold surface, hampering further improvement of the device performance.[17] Thus, inexpensive nanoparticles as a scaffold of porphyrin molecules without such EN quenching are required to improve photocurrent generation efficiency in the composite cluster systems with C_{60}. Silica nanoparticles are potential candidates because of their low cost, nonphotoactive character, and facile functionalization. However, to the best of our knowledge, no silica nanoparticles covalently functionalized with chromophores have been self-organized with acceptor molecules on electrodes resulting in efficient photocurrent generation.[18,19]

We report herein novel photoelectrochemical devices composed of porphyrin-modified silica nanoparticle (Figure 1) and fullerene composite clusters, which are electrophoretically deposited on a nanostructured SnO_2 electrode. The expensive gold core is successfully replaced by a low-cost silica nanoparticle, which would reduce the undesirable EN quenching. Thus, one can expect enhancement of the photocurrent generation efficiency for the porphyrin-modified silica nanoparticle and C_{60} composite system compared with a reference system with a porphyrin-modified gold nanoparticle and C_{60} composite.

Experimental Section

Materials and Methods. C_{60} (99.98%) was obtained from MTR Ltd. Porous nanostructured SnO_2 film was prepared by spraying a dilute (1.5%) SnO_2 colloidal solution (particle size: 15 nm; Chemat Technology, Inc.) on an optically transparent indium−tin oxide electrode (ITO; Tokyo Sanyo Sinku), which was washed by sonicating in 2-propanol and cleaning in O_3 atmosphere in advance, and finally, it was annealed at 673 K for 1 h (denoted as ITO/SnO_2). Activated porphyrin ester **1**,[20] porphyrin reference **4**,[20] and (aminopropyl)silylated silica nanoparticle **2**[21] (Figure 1) were prepared by following the same procedure as described previously. All the other chemicals were of analytical grade and used as received.

* Corresponding author. E-mail: imahori@scl.kyoto-u.ac.jp.
† Department of Molecular Engineering, Kyoto University.
# Fukui Institute for Fundamental Chemistry, Kyoto University.
‡ Institute for Chemical Research, Kyoto University.
¶ Institute of Multidisciplinary Research for Advanced Materials.

10.1021/jp061524+ CCC: $33.50
Published on Web 05/18/2006

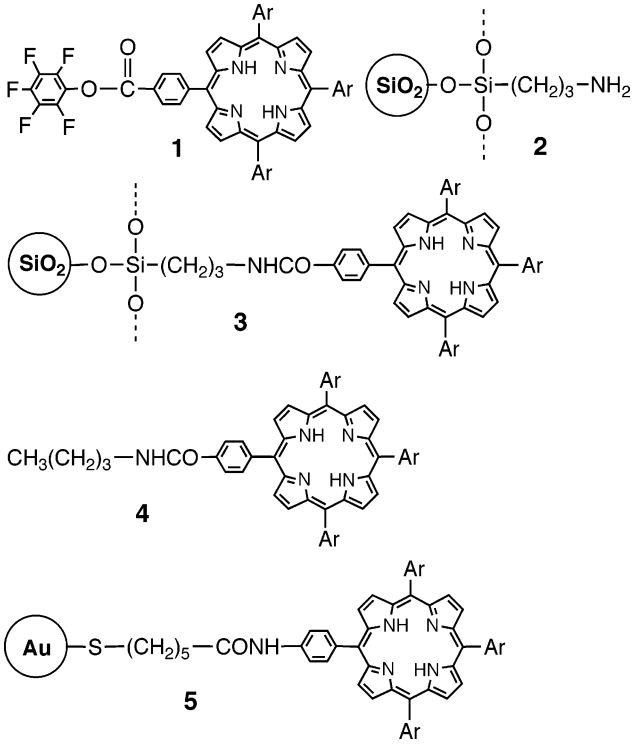

Figure 1. Molecular structures used in this study (Ar = 3,5-(*t*-Bu)$_2$C$_6$H$_3$).

Synthesis and Characterization of Porphyrin-Modified Silica Nanoparticle 3. To a suspension of **2** (100 mg, amino groups of 0.016 mmol) in THF (10 mL) was added at one portion activated porphyrin ester **1**[20] (9.0 mg, 0.0078 mmol), and then the suspended mixture was refluxed for 24 h under nitrogen atmosphere. After cooling, the reaction mixture was centrifuged to give a precipitate, which was washed with THF. The precipitate was dried to afford porphyrin-modified silica nanoparticle **3** as a purple−red solid (85 mg).

An amount of the porphyrin (3.8×10^{-6} mol) chemically adsorbed onto the silica surface in the reaction mixture (10 mL of THF) was determined by comparing the initial and final amounts of the porphyrins in the reaction mixture. This allows us to estimate the extent of porphyrin attachment to amino groups on the silica nanoparticle spectroscopically ($24\% = 100 \times [3.8 \times 10^{-6}/(1.6 \times 10^{-5})]$). Assuming that a molar ratio of the unreacted amino moiety (C_3H_8N) and the porphyrin amido moiety ($C_{72}H_{84}N_5O$) is 1:*x*, a molar ratio of C:N (=(8.11/12.01):(0.93/14.01)) determined from the elemental analysis for **3** (C, 8.11%; H, 1.70%; N, 0.93%) is equal to the following ratio, $(3 + 72x):(1 + 5x)$, yielding $x = 0.33$. Accordingly, the extent of porphyrin attachment to the amino groups on the silica nanoparticle was also estimated as 25% ($=100 \times 0.33/(1 + 0.33)$). A number of amino groups on the surface of one silica nanoparticle was determined as 1.4×10^4 molecules from the comparison of signal intensities of the ^{1}H NMR spectra of **2** for the methyl moiety of DMSO and the methylene moiety of the aminopropyl group.

Preparation of Cluster Solutions and Films. The cluster suspensions of porphyrin-modified silica nanoparticle **3** or the mixture of **3** and C_{60} were prepared in a 1 cm cuvette by injecting 1.0 mL of acetonitrile into a suspension of **3** or **3**−C_{60} in 0.5 mL of toluene (toluene:acetonitrile = 1/2 (v/v)).[13] Two electrodes (ITO and ITO/SnO_2) were kept at a distance of 6 mm using a Teflon spacer and set in the cuvette, and then a dc voltage (500 V) was applied for 2 min between these two electrodes using a power supply (ATTA MODEL AE-8750). The deposition of the film could be confirmed visibly as the solution became colorless.

Characterization. UV−visible absorption spectra of solutions and films on ITO/SnO_2 were recorded using a Lambda 900 spectrophotometer (Perkin-Elmer, USA). ^{1}H NMR spectra were obtained on a JEOL JNM-EX270 using tetramethylsilane as internal standard. Elemental analyses were performed at the Microanalytical Laboratory of Kyoto University. Optical microscopic images were measured by using BX51 microscope (OLYMPUS, Japan). The surface morphology of the films was observed by scanning electron microscopy (SEM) measurements using JSM-6500FE (JEOL, Japan). Transmission electron microscopy (TEM) images were obtained by applying a drop of the sample to a carbon-coated copper grid. Images were recorded with a JEM-200CX transmission electron microscope (JEOL, Japan). Infrared (IR) spectra were recorded in a KBr pellet by using a Spectrometer Lambda 19 (Perkin-Elmer, USA). Time-resolved fluorescence spectra were measured by a single-photon counting method using a second harmonic generation (SHG, 400 nm) of a Ti:sapphire laser (Spectra-Physics, Tsunami 3950-L2S, 1.5 ps fwhm) and a streakscope (Hamamatsu Photonics, C4334-01) equipped with a polychromator (Acton Research, SpectraPro 150) as an excitation source and a detector, respectively.[22]

Photoelectrochemical Measurements. All photoelectrochemical measurements were carried out in a standard three-electrode system using an ALS 630a electrochemical analyzer.[13] The cluster film as a working electrode was contacted onto the electrolyte solution containing 0.5 M LiI and 0.01 M I_2 in acetonitrile, where a Pt wire covered with glass ruggin capillary, whose tip was located near the working electrode, is a reference electrode and a Pt coil is a counter electrode. The potential measured was converted to the saturated calomel electrode (SCE) scale by adding +0.05 V. The stability of the reference electrode potential was confirmed under the experimental conditions. A 500 W xenon lamp (XB-50101AA-A; Ushio, Japan) was used as a light source. The monochromatic light through a monochromator (MC-10N; Ritsu, Japan) was illuminated on the modified area of the working electrode (0.20 cm^2) from the back side. The light intensity was monitored by an optical power meter (ML9002A; Anritsu, Japan) and corrected.

Results and Discussion

Preparation and Characterization of a Porphyrin-Modified Silica Nanoparticle. Activated porphyrin **1**[20] was coupled to (aminopropyl)silylated silica nanoparticle **2**[21] by refluxing for 24 h in toluene to give porphyrin-modified silica nanoparticle **3** (Figure 1). Activated porphyrin **1** also reacted with 1-butylamine to afford porphyrin reference **4**.[20] The structure of **3** was characterized by optical and transmission electron microscopies, absorption and infrared spectroscopies, and elemental analyses. Optical microscopic image of **2** reveals nonstained spheres, whereas that of **3** exhibits purple−red-colored spheres (Figure 2). This indicates that porphyrin molecules are immobilized on the surface of silica nanoparticles **2**. TEM images of **2** and **3** also show spheres with the same average size of 54 nm (Figure 3). The average size of **2** is similar to the value of silica nanoparticle reported previously (50 nm).[21] The identical size and shape of **2** and **3** reveals no occurrence of degradation of the silica nanosphere under the reaction conditions.

To confirm the formation of amide linkage between the porphyrin and the surface of the nanoparticle, IR spectra of **2**−**4**

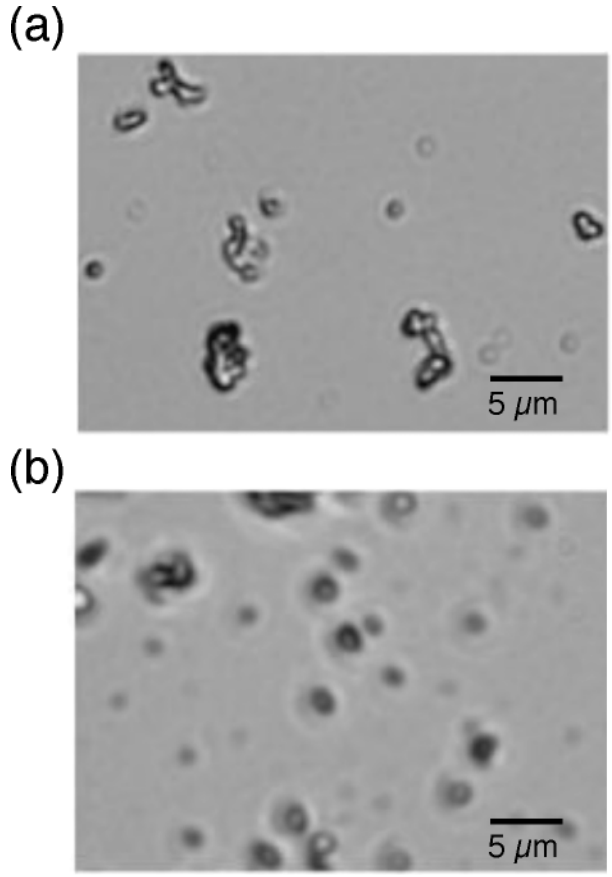

Figure 2. Optical microscopic images of (a) **2** and (b) **3**.

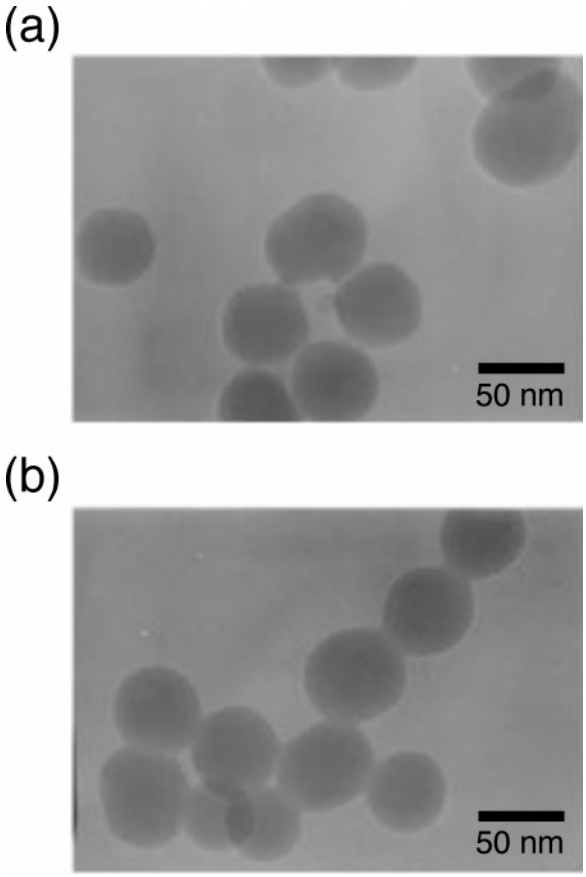

Figure 3. TEM images of (a) **2** and (b) **3**.

were measured in a KBr pellet. Figure 4 displays the IR spectra of **2**−**4** in the wavenumber of 1800−1500 cm^{-1}. The IR spectrum of **2** shows a broad peak at ca. 1660 cm^{-1} arising from the N−H bending vibration of primary amine (Figure 4a), whereas that of **4** reveals peaks at 1671 and 1592 cm^{-1} arising from the C═O stretching vibration of secondary amide and the C═C stretching vibration of phenyl group, respectively (Figure 4c). On the basis of the IR spectra of **2** and **4**, the spectrum of **3** in the wavenumber of 1750−1580 cm^{-1} can be fitted into three component peaks at 1675, 1657, and 1594 cm^{-1}, which are assigned to −CONH, $-NH_2$, and phenyl groups, respectively (Figure 4b). These results support the idea that porphyrin molecules are covalently linked to the surface of the silica nanoparticles.[23]

The extent of porphyrin attachment to amino groups on the silica nanoparticle is estimated as 25% from the elemental analysis for **3** (see Experimental Section). The ratio is consistent with the value (24%) determined from the spectroscopic measurements in which the amounts of the porphyrin chemically adsorbed onto the silica surface can be obtained by comparing the initial and final amounts of the porphyrins in the reaction mixture (see Experimental Section). The occupied area per molecule (Γ) for the porphyrin of **3** is also determined as 3.0 nm^2 ($=4\pi \times (27 + 2)^2/(0.25 \times 1.4 \times 10^4)$) from the extent of the porphyrin functionalization (25%) and the number of amino groups (1.4×10^4 molecules) on the silica nanoparticle of **2** (see Experimental Section).[21] The Γ value is much larger than that for the dense packing of perpendicular porphyrin against the silica surface ($\Gamma = 1.0 \times 2.0 = 2.0$ nm^2). In other words, the average separation distance between the porphyrins on the silica nanoparticle is 1.7 nm, which is much larger than the minimum distance between the porphyrins for the supramolecular incorporation of the C_{60} molecule between the porphyrins.[14] This allows the porphyrins in the silica nanoparticle to bind C_{60} molecules, leading to the formation of porphyrin−C_{60} composites using the silica nanoparticle (vide infra).

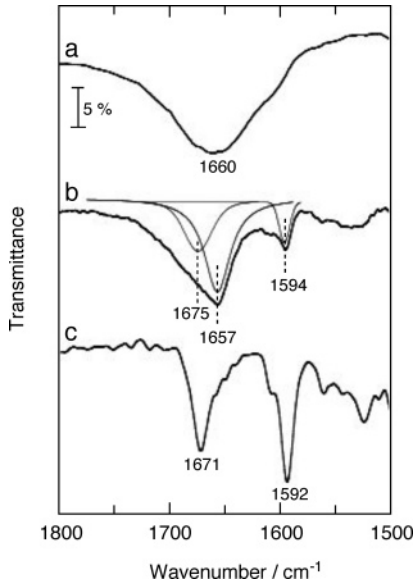

Figure 4. IR spectra of (a) **2**, (b) **3**, and (c) **4** (1500−1800 cm^{-1}) measured in a KBr pellet. The spectrum of **3** in the wavenumber of 1750−1580 cm^{-1} also shows fitted component peaks at 1675, 1657, and 1594 cm^{-1} which are assigned to −CONH, $-NH_2$, and phenyl groups, respectively.

Photophysical Properties of a Porphyrin-Modified Silica Nanoparticle. UV−visible absorption spectra of **3** and **4** were measured in toluene. The λ_{max} value (421 nm) of the Soret band of **3** is the same as that (421 nm) of **4** (Figure 5). This suggests

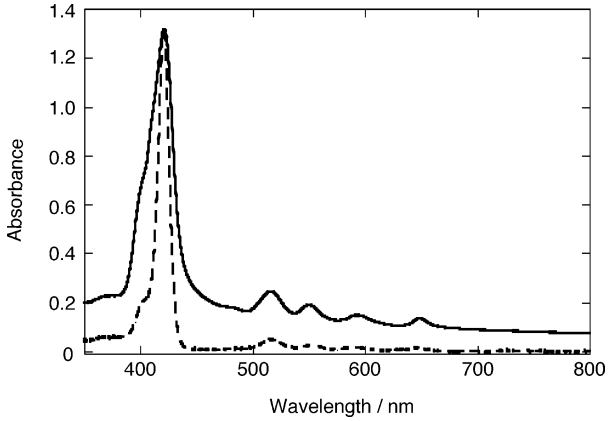

Figure 5. UV−visible absorption spectra of **3** (solid line) and **4** (dotted line, 2.55×10^{-6} M) in toluene. The spectrum of **3** is normalized at the Soret band for comparison.

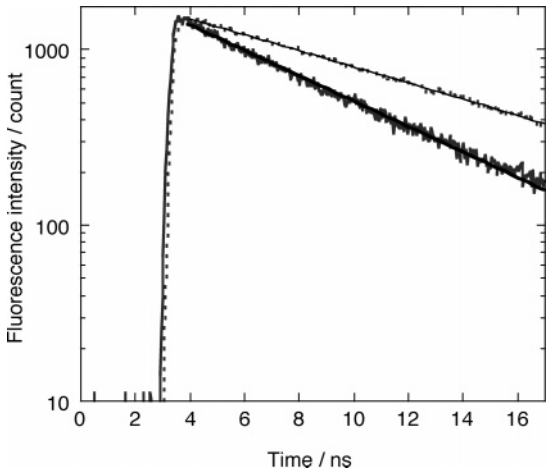

Figure 6. Fluorescence decay curves of **3** (thick line) and **4** (thin line) in toluene at 650 nm (λ_{ex} = 400 nm). They are fitted as a single exponential with lifetimes of 6.2 ns for **3** and 9.6 ns for **4**.

that the porphyrin environment on the silica surface is virtually similar to that in solutions. Steady-state fluorescence spectra were taken in toluene at the excitation of the Soret peak (Figure S1). The absorbance at the Soret peak was adjusted to compare the fluorescence intensity. The fluorescence spectra of **3** and **4** are similar in shape and peak position, but the fluorescence of **3** is moderately reduced relative to that of **4**. To evaluate the lifetime of the porphyrin excited singlet state accurately, the fluorescence lifetime measurements were carried out in toluene at an excitation wavelength (λ_{ex}) of 400 nm. The fluorescence decay curves of **3** and **4** at 650 nm are fitted as a single exponential (Figure 6). The fluorescence lifetime (τ) of **3** (6.2 ns) in toluene is slightly shorter than that of **4** (9.6 ns) in toluene. These results clearly demonstrate that the porphyrins on the silica nanoparticle are not quenched by the silica nanoparticle. This is in sharp contrast with photophysical properties of porphyrin-modified gold nanoparticles in which the porphyrin excited singlet state is quenched strongly by the gold surface through an energy transfer mechanism (**5**: τ = 53 ps (89%), 9.0 ns (11%) in benzene).[17] The slightly shorter fluorescence lifetime of **3** relative to **4** may result from the self-quenching of the porphyrin excited singlet state. Such slow self-quenching of the porphyrin excited singlet state was reported for self-assembled monolayers of similar porphyrins on an ITO electrode, which does not quench the porphyrin excited singlet state.[24]

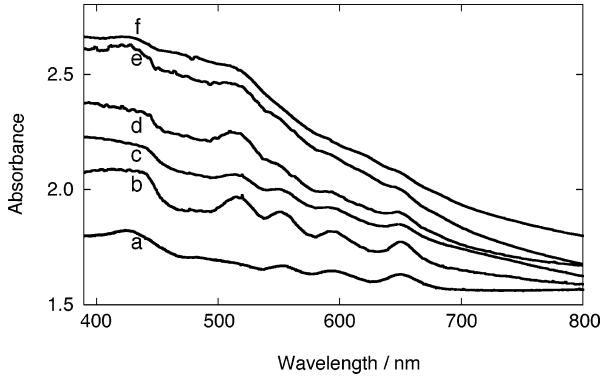

Figure 7. Absorption spectra of ITO/SnO_2/(**3**+C_{60})$_m$: (a) [C_{60}] = 0 mM, (b) 0.08 mM, (c) 0.16 mM, (d) 0.24 mM, (e) 0.32 mM, and (f) 0.40 mM in acetonitrile/toluene = 2/1; [H_2P] = 0.08 mM.

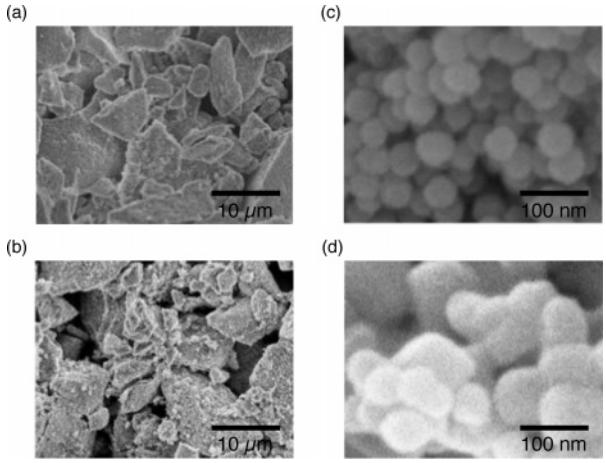

Figure 8. SEM images of ITO/SnO_2/(**3**+C_{60})$_m$: (a) [C_{60}] = 0 mM and (b) [C_{60}] = 0.24 mM in acetonitrile/toluene = 2/1; [H_2P]=0.08 mM. Enlarged (a) and (b) are shown in (c) and (d), respectively.

Formation and Deposition of Composite Clusters. The porphyrin-modified nanoparticle **3** was suspended in toluene containing C_{60}, and they were associated with growing large clusters in an acetonitrile/toluene mixed solvent (denoted as (**3**+C_{60})$_m$).[25] Herein, the concentration of one porphyrin unit in these composite clusters is kept constant in the experiments: [H_2P] = 0.08 mM in acetonitrile/toluene = 2/1, whereas the concentration of C_{60} (0−0.5 mM) is varied in acetonitrile/toluene = 2/1. This procedure allows us to achieve the complex formation between **3** and C_{60} and the larger association at the same time. Then the clusters were attached to nanostructured SnO_2 electrodes by the electrophoretic deposition method (500 V, 2 min) to give the working electrode modified with the composite clusters (denoted as ITO/SnO_2/(**3**+C_{60})$_m$). The light-collecting property of ITO/SnO_2/(**3**+C_{60})$_m$ is found to be intensive in the visible and near-infrared region (Figure 7).[26] SEM images of ITO/SnO_2/(**3**)$_m$ and ITO/SnO_2/(**3**+C_{60})$_m$ electrodes reveal poor packing of large clusters with irregular size and shape on the surface (Figure 8a and b). Nevertheless, the rough surface of the nanoparticles for ITO/SnO_2/(**3**+C_{60})$_m$ (Figure 8d) relative to the smooth surface of the nanoparticles for ITO/SnO_2/(**3**)$_m$ (Figure 8c) demonstrates the formation of the interpenetrating composite clusters of **3** with C_{60} molecules, which are deposited successfully onto the ITO/SnO_2 electrode. Although the nanoparticles with the rough surface are connected with a large excess of C_{60} molecules, incomplete network between the nanoparticles results in the poor formation of the large clusters in micrometer scale (Figure 8b, vide infra).

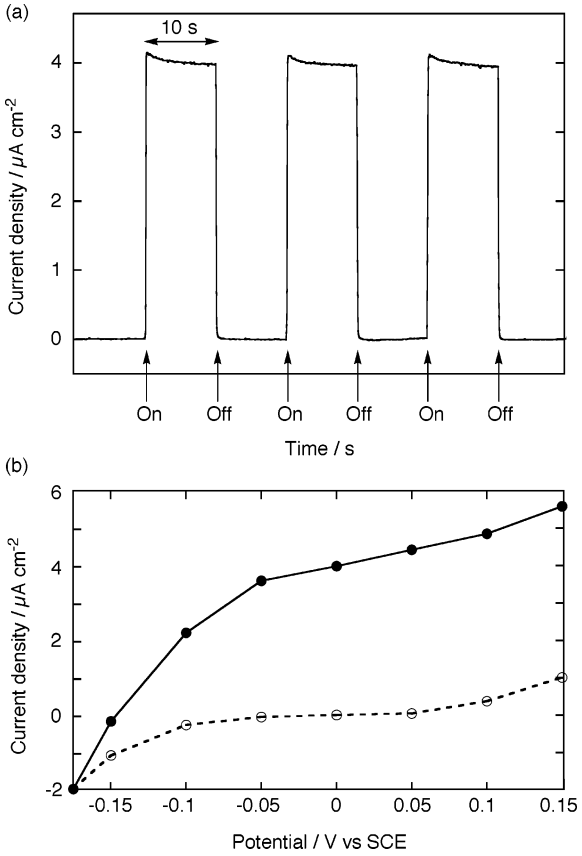

Figure 9. (a) Photocurrent response of ITO/SnO_2/(**3**+C_{60})$_m$ ([**3**] = 0.08 mM, [C_{60}] = 0.32 mM) at λ_{ex} = 420 nm. Potential: +0.05 V vs SCE; 0.5 M LiI and 0.01 M I_2 in acetonitrile. Input power: 125 μW cm^{-2}. (b) Photocurrent versus applied potential curves for ITO/SnO_2/(**3**+C_{60})$_m$ ([**3**] = 0.08 mM, [C_{60}] = 0.32 mM) electrode (solid line with closed circles). The dark currents are shown as a dotted line with open circles; λ = 420 nm (125 μW cm^{-2}); 0.5 M LiI and 0.01 M I_2 in acetonitrile.

Photoelectrochemical Studies. Photoelectrochemical measurements were performed in acetonitrile containing 0.5 M LiI and 0.01 M I_2 with the modified SnO_2 electrode as a working electrode, a platinum counter electrode, and a reference electrode. Figure 9a displays anodic photocurrent responses of SnO_2 electrodes modified with the composite clusters of porphyrin-modified silica nanoparticle **3** and C_{60} (ITO/SnO_2/(**3**+C_{60})$_m$) at an excitation wavelength of 420 nm (input power: 125 μW cm^{-2}) and an applied potential of 0.05 V vs SCE ([**3**] = 0.08 mM, [C_{60}] = 0.32 mM). The photocurrent responses are prompt, steady, and reproducible during repeated on/off cycles of the visible light illumination. The current versus potential characteristics of the ITO/SnO_2/(**3**+C_{60})$_m$ device ([**3**] = 0.08 mM, [C_{60}] = 0.32 mM) was also examined under the same illumination conditions (Figure 9b). With increasing positive bias, the photocurrent increases as compared to the dark current. Increased charge separation and the facile transport of charge carriers under positive bias are responsible for enhanced photocurrent generation.

To evaluate the concentration effect of C_{60} on the photocurrent generation, a series of photocurrent action spectra were recorded and compared against the absorption spectra (Figure 10). IPCE values were calculated by normalizing the photocurrent densities for incident light energy and intensity and using the expression

$$\text{IPCE (\%)} = 100 \times 1240 \times i/(W_{in} \times \lambda)$$

where i is the photocurrent density (A cm^{-2}), W_{in} is the incident light intensity (W cm^{-2}), and λ is the excitation wavelength

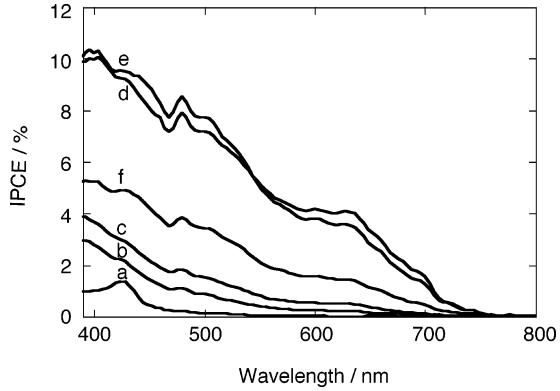

Figure 10. Photocurrent action spectra of ITO/SnO_2/(**3**+C_{60})$_m$ system: (a) [C_{60}] = 0 mM, (b) 0.08 mM, (c) 0.16 mM, (d) 0.24 mM, (e) 0.32 mM, and (f) 0.40 mM in acetonitrile/toluene = 2/1; [H_2P] = 0.08 mM. Applied potential: +0.05 V vs SCE. Electrolyte: 0.5 M LiI, 0.01 M I_2.

(nm). The action spectra largely agree with the absorption spectra on ITO/SnO_2 (Figure 7).[26] The IPCE value initially increases and exhibits 10% as a maximum at 400 nm and finally decreases with increasing the C_{60} concentration (Figure 10).

Taking into account the results of the well-established photodynamic and photoelectrochemical properties of similar porphyrin−fullerene composite devices,[9−13] photocurrent generation in the present system is initiated by photoinduced charge separation or charge transfer from the porphyrin excited singlet state ($^1H_2P^*/H_2P^+ = -1.1$ V vs NHE)[9−13] to C_{60} ($C_{60}/C_{60}^- = -0.2$ V vs NHE)[9−13] in the porphyrin−C_{60} complex rather than direct electron injection into the conduction band of the SnO_2 (0 V vs NHE)[9−13] system. While the reduced C_{60} injects electrons into the SnO_2 nanocrystallites through electron hopping between the C_{60} molecules, the oxidized porphyrin ($H_2P/H_2P^+ = 0.8$ V vs NHE)[9−13] undergoes electron transfer reduction with the iodide ($I_3^-/I^- = 0.5$ V vs NHE)[9−13] in the electrolyte system to generate photocurrent. We and other researchers have previously reported efficient self-exchange electron transfer of porphyrins[27] and fullerenes.[28] Such fast self-exchange electron transfer of porphyrins and fullerenes in the molecular clusters with an interpenetrating network in the thin film results in efficient hopping of hole and electron in each network.

The maximum IPCE value (10%) is 2.5 times as large as that (4%) of the photoelectrochemical device (ITO/SnO_2/(**5**+C_{60})$_m$), comprising the composite clusters of C_{60} and a porphyrin-modified gold nanoparticle whose spacer between the gold surface and the porphyrin is similar to **3**.[12] These results clearly demonstrate that the replacement of a gold core by a silica particle in the porphyrin-modified particles is responsible for the enhancement of photocurrent generation efficiency due to the suppression of undesirable EN quenching of the porphyrin excited singlet state by the silica core in the present system. It is noteworthy that the maximum IPCE value of the ITO/SnO_2/(**3**+C_{60})$_m$ device is rather smaller than that (17%) of the corresponding device using silica microparticles.[19] First, the dead volume of the nanoparticle is much smaller than that of the microparticle. This facilitates the electron and hole transport in the nanoparticle device relative to the microparticle device. Second, both systems exhibit fairly good complexation of the porphyrin-modified particles with C_{60} molecules, leading to ultrafast charge separation in the films. Finally, in the case of nanoparticle system, the small nanoparticles are not connected extensively with a large excess of C_{60} molecules, leading to the poor packing of the large clusters with irregular size and shape on the electrode in micrometer scale (vide supra). In

contrast, porphyrin-modified microparticles are linked with a large excess of C_{60} molecules considerably, resulting in the formation of moderate packing of the large clusters with similar sphere on the electrode in micrometer scale.[19] This raises the electron and hole mobility in the microparticle device compared with the nanoparticle device. Such reverse effects for the two devices may be responsible for the rather similar photoelectrochemical properties of the present device compared with the device using a silica microparticle. The maximum IPCE value of the present system (10%) is also smaller than that of similar porphyrin−fullerene composite system (up to 54%) in which porphyrin-modified gold nanoparticle with a suitably long spacer between the porphyrin and the gold nanoparticle and fullerene are fabricated in the same manner onto the SnO_2 electrode.[12,13] In the latter case, the porphyrin molecules are organized more regularly onto the surface of smaller gold nanoparticles with a diameter of ∼2 nm. The bottom-up fabrication would allow us to form an interpenetrating network of porphyrin and fullerene molecules in the blend film more extensively, leading to the higher performance of the photoelectrochemical device.

Conclusions

In conclusion, we have successfully constructed a photoelectrochemical device comprising porphyrin-modified silica nanoparticles and C_{60} composites for the first time. The maximum IPCE value of the present system (10%) is smaller than that of similar porphyrin−fullerene composite system (up to 54%) in which a porphyrin-modified gold nanoparticle with a suitable spacer and fullerene are fabricated in the same manner onto the SnO_2 electrode. Nevertheless, notable enhancement of the photocurrent generation was achieved in the present system compared with reference system, where a gold core was used as a scaffold of porphyrins instead of a silica nanoparticle.

Acknowledgment. This work was supported by a Grant-in-Aid (No. 11740352 to H.I.) from the Ministry of Education, Culture, Sports, Science and Technology (MEXT), Japan. H.I. also thanks Grant-in-Aid from MEXT, Japan (21st Century COE on Kyoto University Alliance for Chemistry), NEDO, Sekisui Foundation, and Kurata Foundation for financial support. A part of this work was supported by the "Nanotechnology Support Project" of the Ministry of Education, Culture, Sports, Science and Technology (MEXT), Japan. We thank Prof. Tsunehiro Tanaka and Tai Ohuchi (Kyoto University) for the measurements of the IR spectra, and Prof. Susumu Yoshikawa and Junji Aranami (Kyoto University) for the measurements of SEM images.

Supporting Information Available: Steady-state fluorescence spectra (PDF). This material is available free of charge via the Internet at http://pubs.acs.org.

References and Notes

(1) (a) *Organic Photovoltaics*; Sun, S. S., Sariciftci, N. S., Eds.; CRC: Boca Raton, FL, 2005. (b) *Organic Photovoltaics*; Brabec, C., Dyakonov, V., Parisi, J., Sariciftci, N. S., Eds.; Springer: Berlin, 2003.

(2) (a) Tang, C. W. *Appl. Phys. Lett.* **1986**, *48*, 183. (b) Peumans, P.; Yakimov, A.; Forrest, S. R. *J. Appl. Phys.* **2003**, *93*, 3693. (c) Gregg, B. A. *J. Phys. Chem. B* **2003**, *107*, 4688. (d) Coakley, K. M.; McGehee, M. D. *Chem. Mater.* **2004**, *16*, 4533.

(3) (a) Hagfeldt, A.; Grätzel, M. *Acc. Chem. Res.* **2000**, *33*, 269. (b) Bignozzi, C. A.; Argazzi, R.; Kleverlaan, C. J. *Chem. Soc. Rev.* **2000**, *29*, 87. (c) Lewis, N. S. *Inorg. Chem.* **2005**, *44*, 6900. (d) Badaranayake, K. M. P.; Senevirathna, M. K. I.; Weligamuwa, P. M. G. M. P.; Tennakone, K. *Coord. Chem. Rev.* **2004**, *248*, 1277. (e) Ito, S.; Kitamura, T.; Wada, Y.; Yanagida, S. *Solar Energy Mater. Solar Cell* **2003**, *76*, 3. (f) Ushiroda, S.; Ruzycki, N.; Lu, Y.; Spitler, M. T.; Parkinson, B. A. *J. Am. Chem. Soc.* **2005**, *127*, 5158.

(4) (a) Hirata, N.; Lagref, J.-J.; Palomares, E. J.; Durrant, J. R.; Nazeeruddin, M. K.; Grätzel, M.; Di Censo, D. *Chem.—Eur. J.* **2004**, *10*, 595. (b) Piotrowiak, P.; Galoppini, E.; Wei, Q.; Meyer, G. J.; Wiewior, P. *J. Am. Chem. Soc.* **2003**, *125*, 5278. (c) Kamat, P. V.; Haria, M.; Hotchandani, S. *J. Phys. Chem. B* **2004**, *108*, 5166. (d) Benkö, G.; Myllyperkiö, P.; Pan, J.; Yartsev, A. P.; Sundström, V. *J. Am. Chem. Soc.* **2003**, *125*, 1118. (e) Asbury, J. B.; Ellingson, R. J.; Ghosh, H. N.; Ferrere, S.; Nozik, A. J.; Lian, T. *J. Phys. Chem. B* **1999**, *103*, 3110. (f) Katoh, R.; Furube, A.; Barzykin, A. V.; Arakawa, H.; Tachiya, M. *Coord. Chem. Rev.* **2004**, *248*, 1195.

(5) (a) Yu, G.; Gao, J.; Hummelen, J. C.; Wudl, F.; Heeger, A. J. *Science* **1995**, *270*, 1789. (b) Padinger, F.; Rittberger, R. S.; Sariciftci, N. S. *Adv. Funct. Mater.* **2003**, *13*, 85. (c) Wienk, M. M.; Kroon, J. M.; Verhees, W. J. H.; Knol, J.; Hummelen, J. C.; van Hal, P. A.; Janssen, R. A. J. *Angew. Chem. Ind. Ed.* **2003**, *42*, 3371. (d) Ma, W.; Yang, C.; Gong, X.; Lee, K.; Heeger, A. J. *Adv. Funct. Mater.* **2005**, *15*, 1617. (e) Riedel, I.; von Hauff, E.; Parisi, J.; Martín, N.; Giacalone, F.; Dyakonov, V. *Adv. Funct. Mater.* **2005**, *15*, 1979. (f) Li, G.; Shrotriya, V.; Huang, J.; Yao, Y.; Moriarty, T.; Emery, K.; Yang, Y. *Nat. Mater.* **2005**, *4*, 864.

(6) (a) Halls, J. J. M.; Walsh, C. A.; Greenham, N. C.; Marseglia, E. A.; Friend, R. H.; Moratti, S. C.; Holmes, A. B. *Nature* **1995**, *376*, 498. (b) Schmidt-Mende, L.; Fechtenkötter, A.; Müllen, K.; Moons, E.; Friend, R. H.; MacKenzie, J. D. *Science* **2001**, *293*, 1119. (c) Nierengarten, J.-F. *New J. Chem.* **2004**, *28*, 1177. (d) Arango, A. C.; Johnson, L. R.; Bliznyuk, V. N.; Schlesinger, Z.; Carter, S. A.; Hörhold, H.-H. *Adv. Mater.* **2000**, *12*, 1689.

(7) (a) Hiramoto, M.; Fujiwara, H.; Yokoyama, M. *Appl. Phys. Lett.* **1991**, *58*, 1062. (b) Tsuzuki, T.; Shirota, Y.; Rostalski, J.; Meissner, D. *Solar Energy Mater. Solar Cells* **2000**, *61*, 1. (c) Xue, J.; Uchida, S.; Rand, B. P.; Forrest, S. R. *Appl. Phys. Lett.* **2004**, *84*, 3013.

(8) (a) Huynh, W. U.; Dittmer, J. J.; Alivisatos, A. P. *Science* **2002**, *295*, 2425. (b) Liu, J.; Tanaka, T.; Sivula, K.; Alivisatos, A. P.; Fréchet, J. M. J. *J. Am. Chem. Soc.* **2004**, *126*, 6550.

(9) (a) Imahori, H. *J. Phys. Chem. B* **2004**, *108*, 6130. (b) Imahori, H.; Fukuzumi, S. *Adv. Funct. Mater.* **2004**, *14*, 525.

(10) (a) Hasobe, T.; Kashiwagi, Y.; Absalom, M. A.; Sly, J.; Hosomizu, K.; Crossley, M. J.; Imahori, H.; Kamat, P. V.; Fukuzumi, S. *Adv. Mater.* **2004**, *16*, 975. (b) Hasobe, T.; Kamat, P. V.; Absalom, M. A.; Kashiwagi, Y.; Sly, J.; Crossley, M. J.; Hosomizu, K.; Imahori, H.; Fukuzumi, S. *J. Phys. Chem. B* **2004**, *108*, 12865.

(11) Hasobe, T.; Kamat, P. V.; Troiani, V.; Solladié, N.; Ahn, T. K.; Kim, S. K.; Kim, D.; Kongkanand, A.; Kuwabata, S.; Fukuzumi, S. *J. Phys. Chem. B* **2005**, *109*, 19.

(12) (a) Hasobe, T.; Imahori, H.; Kamat, P. V.; Fukuzumi, S. *J. Am. Chem. Soc.* **2003**, *125*, 14962. (b) Hasobe, T.; Imahori, H.; Kamat, P. V.; Ahn, T. K.; Kim, S. K.; Kim, D.; Fujimoto, A.; Hirakawa, T.; Fukuzumi, S. *J. Am. Chem. Soc.* **2005**, *127*, 1216.

(13) (a) Imahori, H.; Fujimoto, A.; Kang, S.; Hotta, H.; Yoshida, K.; Umeyama, T.; Matano, Y.; Isoda, S. *Adv. Mater.* **2005**, *17*, 1727. (b) Imahori, H.; Fujimoto, A.; Kang, S.; Hotta, H.; Yoshida, K.; Umeyama, T.; Matano, Y.; Isoda, S.; Isosomppi, M.; Tkachenko, N. V.; Lemmetyinen, H. *Chem.—Eur. J.* **2005**, *11*, 7265. (c) Imahori, H.; Fujimoto, A.; Kang, S.; Hotta, H.; Yoshida, K.; Umeyama, T.; Matano, Y.; Isoda, S. *Tetrahedron* **2006**, *62*, 1955.

(14) (a) Evans, D. R.; Fackler, N. L. P.; Xie, Z.; Rickard, C. E. F.; Boyd, P. D. W.; Reed, C. A. *J. Am. Chem. Soc.* **1999**, *121*, 8466. (b) Sun, D.; Tham, F. S.; Reed, C. A.; Chaker, L.; Boyd, P. D. W. *J. Am. Chem. Soc.* **2002**, *124*, 6604. (c) Tashiro, K.; Aida, T.; Zheng, J.-Y.; Kinbara, K.; Saigo, K.; Sakamoto, S.; Yamaguchi, K. *J. Am. Chem. Soc.* **1999**, *121*, 9477. (d) Imahori, H.; Hagiwara, K.; Aoki, M.; Akiyama, T.; Taniguchi, S.; Okada, T.; Shirakawa, M.; Sakata, Y. *J. Am. Chem. Soc.* **1996**, *118*, 11771. (e) Shirakawa, M.; Fujita, N.; Shinkai, S. *J. Am. Chem. Soc.* **2003**, *125*, 9902.

(15) (a) Kamat, P. V.; Barazzouk, S.; Thomas, K. G.; Hotchandani, S. *J. Phys. Chem. B* **2000**, *104*, 4014. (b) Kamat, P. V.; Haria, M.; Hotchandani, S. *J. Phys. Chem. B* **2004**, *108*, 5166. (c) Kamat, P. V.; Barazzouk, S.; Hotchandani, S.; Thomas, K. G. *Chem.—Eur. J.* **2000**, *6*, 3914.

(16) Gold nanoparticles have been employed to assemble photoactive molecules on electrode surfaces for photoelectrochemical devices, but the photocurrent generation efficiencies are much lower than that in the present system. See: (a) Kuwahara, Y.; Akiyama, T.; Yamada, S. *Langmuir* **2001**, *17*, 5714. (b) Sudeep, P. K.; Ipe, B. I.; Thomas, K. G.; George, M. V.; Barazzouk, S.; Hotchandani, S.; Kamat, P. V. *Nano Lett.* **2002**, *2*, 29. (c) Thomas, K. G.; Kamat, P. V. *Acc. Chem. Res.* **2003**, *36*, 888. (d) Kamat, P. V. *J. Phys. Chem. B* **2002**, *106*, 7729. (e) Lahav, M.; Heleg-Shabtai, V.; Wasserman, J.; Katz, E.; Willner, I.; Durr, H.; Hu, Y. Z.; Bossmann, S. H. *J. Am. Chem. Soc.* **2000**, *122*, 11480. (f) Lahav, M.; Gabriel, T.; Shipway, A. N.; Willner, I. *J. Am. Chem. Soc.* **1999**, *121*, 258.

(17) (a) Imahori, H.; Arimura, M.; Hanada, T.; Nishimura, Y.; Yamazaki, I.; Sakata, Y.; Fukuzumi, S. *J. Am. Chem. Soc.* **2001**, *123*, 335. (b) Imahori, H.; Kashiwagi, Y.; Hanada, T.; Endo, Y.; Nishimura, Y.; Yamazaki, I.;

Fukuzumi, S. *J. Mater. Chem.* **2003**, *13*, 2890. (c) Fukuzumi, S.; Endo, Y.; Kashiwagi, Y.; Araki, Y.; Ito, O.; Imahori, H. *J. Phys. Chem. B* **2003**, *107*, 11979. (d) Imahori, H.; Kashiwagi, Y.; Endo, Y.; Hanada, T.; Nishimura, Y.; Yamazaki, I.; Aaraki, Y.; Ito, O.; Fukuzumi, S. *Langmuir* **2004**, *20*, 73.

(18) (a) Furukawa, H.; Inoue, N.; Watanabe, T.; Kuroda, K. *Langmuir* **2005**, *21*, 3992. (b) Li, G.; Bhosale, S. V.; Wang, T.; Hackbarth, S.; Roeder, B.; Siggel, U.; Fuhrhop, J. H. *J. Am. Chem. Soc.* **2003**, *125*, 10693. (c) Yui, T.; Tsuchino, T.; Itoh, T.; Ogawa, M.; Fukushima, Y.; Takagi, K. *Langmuir* **2005**, *21*, 2644. (d) Han, B.-H.; Manners, I.; Winnik, M. A. *Chem. Mater.* **2005**, *17*, 3160.

(19) A porphyrin-modified silica microparticle−C_{60} composite photoelectrochemical device has been reported to exhibit efficient photocurrent generation compared with a similar photoelectrochemical device using a gold nanoparticle. See: Imahori, H.; Mitamura, K.; Umeyama, T.; Hosomizu, K.; Matano, Y.; Yoshida, K.; Isoda, S. *Chem. Commun.* **2006**, 406.

(20) Imahori, H.; Hosomizu, K.; Mori, Y.; Sato, T.; Ahn, T. K.; Kim, S. K.; Kim, D.; Nishimura, Y.; Yamazaki, I.; Ishii, H.; Hotta, H.; Matano, Y. *J. Phys. Chem. B* **2004**, *108*, 5018.

(21) Hiramatsu, H.; Osterloh, F. E. *Langmuir* **2003**, *19*, 7003.

(22) Yamazaki, M.; Araki, Y.; Fujitsuka, M.; Ito, O. *J. Phys. Chem. A* **2001**, *105*, 8615.

(23) Although ^{1}H NMR signals of **2** appeared in DMSO-d_6,[21] that of **3** could not be obtained because of the relatively low solubility and extensive broadening of the NMR signals characteristic of immobilized molecules on nanoparticles.[17]

(24) (a) Yamada, H.; Imahori, H.; Nishimura, Y.; Yamazaki, I.; Fukuzumi, S. *Adv. Mater.* **2002**, *14*, 892. (b) Yamada, H.; Imahori, H.; Nishimura, Y.; Yamazaki, I.; Ahn, T. K.; Kim, S. K.; Kim, D.; Fukuzumi, S. *J. Am. Chem. Soc.* **2003**, *125*, 14962.

(25) Charge transfer absorption arising from the complexation between porphyrin and C_{60} could not be confirmed in toluene and toluene−acetonitrile mixtures because of the relatively low solubility of the porphyrin-modified nanoparticle **3**.

(26) The absorption spectra of the clusters on ITO/SnO_2 include the scattering of the incident light by the nanometer-sized SnO_2 particles and the composite clusters. Such an effect may be responsible for the small difference in the absorption spectra on ITO/SnO_2 and the action spectra (vide infra).

(27) (a) Fukuzumi, S.; Endo, Y.; Imahori, H. *J. Am. Chem. Soc.* **2002**, *124*, 10974. (b) Fukuzumi, S.; Hasobe, T.; Endo, Y.; Kei Ohkubo, K.; Imahori, H. *J. Porphyrins Phthalocyanines* **2003**, *7*, 328. (c) Crnogorac, M. M.; Kostic, N. M. *Inorg. Chem.* **2000**, *39*, 5028. (d) Sun, H.; Smirnov, V. V.; DiMagno, S. G. *Inorg. Chem.* **2003**, *42*, 6032.

(28) (a) Fukuzumi, S.; Nakanishi, I.; Suenobu, T.; Kadish, K. M. *J. Am. Chem. Soc.* **1999**, *121*, 3468. (b) Thomas, K. G.; Biju, V.; Guldi, D. M.; Kamat, P. V.; George, M. V. *J. Phys. Chem. B* **1999**, *103*, 8864.